Dyes and Pigments 220 (2023) 111754

Contents lists available at ScienceDirect

Dyes and Pigments

journal homepage: www.elsevier.com/locate/dyepig

Diphenyl ditelluride assisted synthesis of noble metal-based silver-telluride 2D organometallic nanofibers with enhanced aggregation-induced emission (AIE) after oleylamine treatment

Jamila Djafari [a], Frederico Duarte [a,b], Javier Fernández-Lodeiro [a,b,**], Adrián Fernández-Lodeiro [a,b], Hugo Santos [a,b], Eva Bladt [c,d], Sara Bals [c,d], Aikaterini Flessa Savvidou [e,f], Luis Balicas [e,f], Benito Rodríguez-González [g,h], Alcindo Aparecido Dos Santos [i], José Luis Capelo-Martínez [a,b], Carlos Lodeiro [a,b,*]

[a] BIOSCOPE Research Group, LAQV-REQUIMTE, Chemistry Department, NOVA School of Science and Technology, Universidade NOVA de Lisboa, 2829-516, Caparica, Portugal
[b] PROTEOMASS Scientific Society, BIOSCOPE Research GROUP, Departmental Building, Ground Floor, FCT-UNL Caparica Campus, 2829-516, Caparica, Portugal
[c] Electron Microscopy for Materials Science (EMAT), University of Antwerp, Groenenborgerlaan 171, Antwerp, 2020, Belgium
[d] NANOlab Center of Excellence, University of Antwerp, Groenenborgerlaan 171, Antwerp, 2020, Belgium
[e] National High Magnetic Field Laboratory, Tallahassee, FL, 32310, USA
[f] Department of Physics, Florida State University, Tallahassee, FL, 32306, USA
[g] CINBIO, Universidade de Vigo, Departamento de Química Física, Campus Universitario Lagoas Marcosende, 36310, Vigo, Spain
[h] Galicia Sur Health Research Institute (IIS Galicia Sur), SERGAS-UVIGO, 36310, Vigo, Spain
[i] Departamento de Química Fundamental, Instituto de Química, Universidade de São Paulo, SP, São Paulo, Brazil

ARTICLE INFO

Keywords:
Tellurium
Silver
Nanofiber
Oleylamine
Fluorescence

ABSTRACT

Silver-Telluride 2D organometallic nanofibers (NFs), using diphenyl ditelluride (DPDT) as a precursor, were synthesized. The synthesis was carried out by reacting DPDT with $AgNO_3$ in acetonitrile at room temperature (RT) under an inert atmosphere. The resulting material was fully characterized using various techniques, including UV-VIS-NIR spectroscopy, steady-state and excited-state fluorescence spectroscopy, IR-FTIR-ATR spectroscopy, HR-ESI MS spectrometry, high-resolution transmission electron microscopy (HRTEM), BF-STEM or HAADF-STEM, confocal fluorescence microscopy images and conductivity measurements. Initially, the nanofibers were almost non-emissive. However, a remarkable modification was observed after treating the nanofibers with oleylamine under ultrasound treatment. This methodology induced an aggregation emission effect (AIE) in the solution and in the solid state, resulting in the formation of a highly red emissive fluorescent nanomaterial. This research provides valuable insights for developing new fluorescent materials with potential applications in various optical fields.

1. Introduction

Diorganyl ditellurides (RTe−TeR) have emerged as a versatile precursor for synthesizing various metal telluride nanomaterials and nanocrystal ligands, attracting significant attention from the scientific community· [1] The relatively weak Te–Te bonds present in diorganyl ditellurides can be easily cleaved under mild thermolytic or photolytic conditions, making them suitable for manufacturing different metal-telluride or telluride nanocrystals such as CdTe [2], SnTe [3], tellurium nanorods [4], and others, via either solvothermal, photolytic, or vapour deposition processes.

Of particular interest are tellurium-containing silver materials, which have potential applications in harvesting thermal and mechanical energy as well as in the production of insulator materials. These

* Corresponding author. BIOSCOPE Research Group, LAQV-REQUIMTE, Chemistry Department, NOVA School of Science and Technology, Universidade NOVA de Lisboa, 2829-516, Caparica, Portugal.
** Corresponding author. BIOSCOPE Research Group, LAQV-REQUIMTE, Chemistry Department, NOVA School of Science and Technology, Universidade NOVA de Lisboa, 2829-516, Caparica, Portugal.
E-mail addresses: j.lodeiro@fct.unl.pt (J. Fernández-Lodeiro), cle@fct.unl.pt (C. Lodeiro).

https://doi.org/10.1016/j.dyepig.2023.111754
Received 4 September 2023; Received in revised form 6 October 2023; Accepted 8 October 2023
Available online 10 October 2023

materials offer unique optical and electronic properties that make them highly attractive for use in various fields, including electronics, photonics, and renewable energy [5,6].

Overall, the use of diorganyl ditellurides as a precursor for the synthesis of metal telluride nanomaterials and nanocrystal is a promising area of research. Further research in this area will likely yield valuable insights into the properties and potential applications of these materials.

In the field of coordination chemistry, RTe- TeR species are promising ligands due to their bonding flexibility, redox properties, and multidenticity. They can be used to fabricate metal or metal chalcogenide nanomaterials using relatively softer chemical routes. For example, our group has reported on the ability of diphenyl ditelluride (DPDT) to reduce Au(III) into well-defined spherical gold nanoparticles (AuNPs) in acetonitrile solution at room temperature. This process occurs via Te–Te oxidative cleavage with the concomitant formation of gold nanoparticles and halogenated tellurium derivatives as a subproduct. Controlled oxo-hydrolysis of such halogenated entities and photodecomposition of DPDT generate an oligomeric organotellurium structure deposited over the gold cores, leading to highly stable core@shell nanoparticles [7].

In addition to gold, platinum (IV) can also be used as a metal precursor in the presence of diorganyl ditelluride derivatives. Partial reduction of Pt(IV) generates highly monodisperse Pt–Te organometallic nanoparticles, which can be used as a single-source precursor to manufacture well-defined $PtTe_2$ multi-crystal nanoparticles under a solvothermal process [8].

In summary, the use of diorganyl ditellurides in coordination chemistry opens a promising field of investigation that can lead to the development of novel and efficient routes for synthesizing metal and metal chalcogenide nanomaterials.

The reaction of Ag(I) with diorganyl ditellurides was reported several years ago [9]. It resulted in the formation of organometallic dimers or polymers when different diorganyl ditellurides were reacted with AgBF4. In the case of DPDT, the authors described the spontaneous formation of an organometallic polymer, indicating the high reactivity of DPDT towards Ag(I). However, the product partially decomposed under vacuum at ambient temperature, which hindered further characterization.

Materials producing aggregation-induced emission (AIE) are very interested in industrial and technological applications. AIE is a fascinating photophysical phenomenon that has attracted significant attention in recent years. Unlike traditional luminophores, which often exhibit decreased luminescence upon aggregation, AIE materials become highly emissive when aggregated or in the solid state. This process is intriguing and has revolutionized our understanding of how aggregation affects luminescence [10].

One significant advantage of AIE materials is their use in designing more sophisticated fluorescent probes for detecting biological targets, including proteins, nucleic acids, or small molecules [11,12]. AIE materials have also shown promising potential in optoelectronic applications such as organic light-emitting diodes (OLEDs) and organic photovoltaics (OPVs) [13]. Their unique properties, such as high quantum yield and efficient energy transfer, make them suitable for these applications.

Moreover, AIE materials have attracted significant interest in the field of green energy, particularly in the design of luminescent solar concentrators (LSCs). These materials can efficiently absorb and convert sunlight into electricity and have potential applications in building-integrated photovoltaics and portable devices [14]. Further research in this area is expected to yield valuable insights and lead to the development of novel AIE materials with enhanced photophysical properties and expanded applications.

Following our interest in developing new synthetic routes based on organic ditellurides to prepare noble metal-based nanomaterials, we explore the reactivity of DPDT with $AgNO_3$ in acetonitrile at room temperature under inert atmosphere. Early, W.-F. Liaw and co-workers investigated the interaction of diorganyl ditellurides in a molar relation Ag/Te–Te of 1/2 or 1/3 [9]. In our case, the reaction was adjusted to start with a molar ratio Ag(I)/DPDT 1/0.55 using acetonitrile as the solvent under inert atmosphere. In a representative experiment, a fresh prepared solution of DPDT in acetonitrile was injected into an acetonitrile solution of $AgNO_3$ at room temperature. The solution acquires an initial red colour that, after stirring for 30 min, evolves into forming a garnet precipitate with a fibrillar aspect. A stable garnet solution was obtained upon purification in acetonitrile using centrifugation, which did not precipitate even after several days in the solution.

High-resolution transmission electron microscopy (HR-TEM) analysis was performed to characterize the material (Fig. 1A). The HR-TEM analysis revealed the formation of long nanofibers (NFs) with thicknesses of 10–20 nm and with intricate nano structure (Fig. 1B). Interestingly, we observed an evident alignment of internal granular electron-dense nanostructures of 1.5–2 nm along the fibber and separated by a channel of about 3.5 nm (See Figure S1A, B), which are more pronounced in the Bright Field Scanning Transmission Electron Microscopy (BF-STEM) or Annular dark-field imaging - Scanning Transmission Electron Microscopy (HAADF-STEM) images shown in Fig. 1C and D. Albeit the dark areas, related to the higher atomic number elements (Ag and Te), did not show crystal phases observed in the HR-TEM images (See Figure S1C), the electron diffraction (ED) showed a pattern of rings that can be related to the formation of really small crystallites with planes not yet very well defined, or small crystalline nanoclusters (Fig. 1E).

However, unfortunately, the organometallic nanofibers (denoted as AgTe NFs) showed limited electron beam stability during microscopy studies. HAADF-STEM investigation at 120 and 300 kV showed that the nanofibers degrade upon electron beam scanning after $t > 10$ s (see Figure S2), which limited our ability to accurately determine their structure. Based on the EDX spectrum, the composition was found *ca.* 53 % of Ag and *ca.* 47 % of Te (see Figure S3).

The UV-VIS absorption spectrum of the AgTe NFs in acetonitrile solution showed two intense absorption peaks centered at *ca.* 476 nm and 562 nm with comparable relative intensities (Fig. 1F). To further investigate the origin of the observed bands, spectroscopy measurements of the DPDT in acetonitrile were performed. Initially, its solution presents an absorption peak at *ca.* 397 nm corresponding to the transition $nTe-\sigma^*$ (Te–Te CT band) [7]. After reaction with the silver salt, the formation of two absorption bands at low energy was observed (see Figure S4). Although the peak at 476 nm could be related to the formation of a metal complex between Ag(I) and DPDT, the peak observed at lower energy (562 nm) is reminiscent of discrete energy levels in quantum confined nanocrystals, albeit a residual fluorescent emission was observed.

In our previous work on the reactivity of DPDT with Au(III), we have observed the formation of a coordinated organometallic complex $[Au(DPDT)_2]^+$ after a partial reduction of Au(III) to Au(I) mediated by the Te–Te moiety, that subsequently evolves towards metallic AuNPs [7]. Here, since crystal phases were not discernible in the electron microscopy images, the absorption at 562 nm is less likely to be attributed to either plasmonic effects from silver NPs or band gap absorption in the semiconductor nanocrystals and should be associated with a transition band.

To further investigate the formation of the AgTe NFs, electrospray ionization mass spectrometry (ESI-MS) was performed during the reaction. As shown in Figure S5, after *ca.* one minute of reaction, the two more intense signals at 518.791 and 928.678 *m/z* can be assigned to the formation of the monometallic complexes $[(Ph_2Te_2)Ag]^+$ and $[(Ph_2Te_2)_2Ag]^+$ (theoretical mass of: 518.793 and 928.681 *m/z* respectively. With the progress of the reaction (*ca.* 5 min), some structures at a higher *m/z* ratio indicate the evolution of the monometallic complexes (see Figure S6).

For example, the signal at 1847.245 *m/z* can be assigned to the tetra metallic multicentre complexes, such as $[(Ph_2Te_2)_3Ag_4(NO_3)_3]^+$

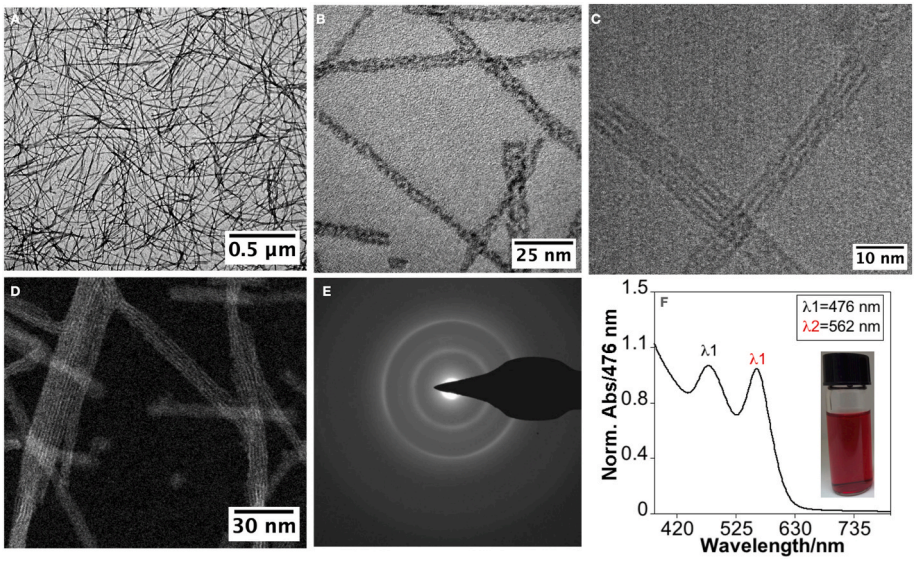

Fig. 1. HRTEM images (A, B), bright-field STEM (C), HAADF-STEM (D) and electron diffraction pattern (E) of the AgTe NFs. Absorption spectra (F) of purified AgTe NFs in acetonitrile (inset in panel F shows the colour colloidal suspension of AgTe NFs).

(theoretical calc. mass of 1847.246 *m/z*). If we consider the preferential coordination of silver centres (n_c = 2) and based on the complexes observed in the mass spectrometry analysis and the alignment of the dark areas (Ag and Te) with lighter separation channels (related with atoms of low atomic number). It seems reasonable to propose that the formation of the 2D organometallic nanofibers could be originated from the spontaneous rearrangement directed by the coordination of Ag(I) towards Te atoms. The phenyl group seems to be allocated around the coordination chain which can contribute to stabilize the fibrillar-like nanostructure by π-π interactions between the rings.

Furthermore, the FTIR-ATR confirmed the presence of phenyl groups in the nanostructure (see Figure S7). The signals at 1570 cm^{-1}, 1470 cm^{-1}, 1432 cm^{-1} can be attributed to (C═C stretches), 1014 cm^{-1} to the C–H bending in-plane, C–H bending out-of-plane (726 cm^{-1}, 687 cm^{-1}) [8] and ν(Te–C) (453 cm^{-1}) [15]. Moreover, the spectra shows a very narrow peak at *ca* 1353 cm^{-1} that could be attributed to the ionic nitrate group in metal complexed materials (see Figure S7) [16].

Some tellurium containing materials are known to be

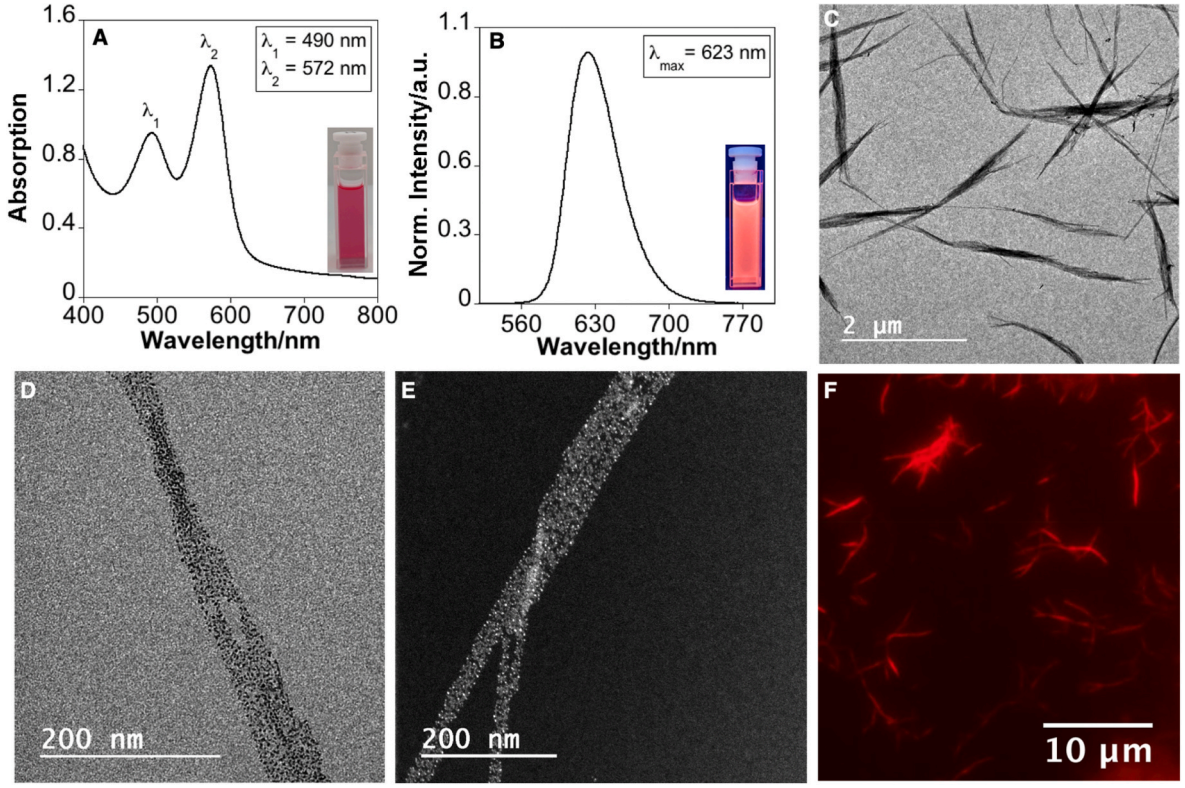

Fig. 2. Absorption (A) and fluorescence emission (B) spectra of purified fluorescence OAm-AgTe NFs in hexane. λ_{exc} = 490 nm (inset in panel A and B shows the colour solution under normal and UV light respectively, λ_{exc} = 365 nm). TEM (C, D), HAADF-STEM (E) and confocal fluorescence images (F) of the OAm-AgTe NFs nanofibers.

semiconductors, and it is well-documented how the electrical resistance of tellurium decreases with the addition of a few atoms of copper and antimony [17–19]. To evaluate the conductivity of the AgTe NFs, several studies were performed. The conductivity was assessed through a quasi-DC transport method. The dried AgTe NFs powder were pressed into a pellet having a diameter of 3 mm and a thickness of 0.5 mm. This pellet was subsequently cut into bars having a width of approximately 1.5 mm. Electrical contacts to Pt wires were attached using Ag paint (Dupont 4929 N) in a four-terminal configuration. A current source meter (Keithley 6221) was used to inject a continuous current whose sign was periodically flipped, and the voltage was measured in Delta mode via a nanovoltmeter (Keithley 2182a). At room temperature, the resistance of the pellet was strongly current-dependent, stabilizing at a value of ~7 GW cm when the current was reduced to 50 picoA. This resistivity value should be taken as a lower bound since further decreasing the current leads to strong fluctuations in the measured value, implying that it might be higher. Therefore, the AgTe NFs are strongly insulating at room temperature, mainly due to the phenyl groups that cover the Ag–Te channels.

Being the AgTe NFs almost non-emissive materials, we designed a treatment with oleylamine (OAm) under ultrasound energy (ultrasonic bath operating at 35 kHz) resulting in a highly emissive fluorescent solution.

As shown in Fig. 2A, the interaction of OAm with the nanofibers (denoted as OAm-AgTe NFs) resulted in a 14 nm redshift of the absorption peak at higher energy. The absorption band at lower energy exhibited a 10 nm redshift with increased intensity compared to untreated NFs (see Fig. 1F). Interestingly, it exhibited strong emission with a fluorescence band centered at *ca.* 623 nm when excited at 490 nm (Fig. 2B).

HR-TEM and HAADF-STEM studies showed that the OAm-AgTe NFs exhibited dark regions randomly dispersed along the nanofiber, rather than an aligned distribution as observed in the untreated NFs (Fig. 2 C-E and Figure S8 A-C).

It can be noted that, similar to the AgTe NFs, no clear crystal phase were observed in the OAm-AgTe NFs upon inspection at higher magnifications using HR-TEM (see Figure S8 D-F) Resembling the initial organometallic nanofibers, where the electron beam irradiation led to the degradation of the nanostructure, now, curiously, certain regions of the nanofibers showed a rapid crystal growth upon exposure to the electron beam (see Figure S9).

Confocal fluorescence microscopy imaging studies revealed that the fluorescence emission is originated from the NFs rather than a discrete nanostructure isolated from the nanofibers (see Fig. 2F).

The XPS analysis validates the composition of AgTe nanofibers (NFs) as determined from the EDS spectrum. It reveals an atomic ratio of Ag: Te, which is 13:12 for AgTe NFs and 6.5:6 for OAm-AgTe NFs. The similarity in atomic percentages in both cases suggests that there was no Te or Ag extrusion from the nanofibers after treatment with OAm. In the Te3d region, the AgTe NFs exhibit a strong signal at 573.6 eV, which can be associated with the organic Tellurium content within the NFs [20, 21]. Additionally, the presence of a second component at 576.0 eV (see Figure S10) can be attributed to the partial oxidation of certain Te atoms [18]. Moving to the Ag3d region, the AgTe NFs display a peak from $Ag3d_{5/2}$ at 368.9 eV, which can be originated from Ag(I) [22,23]. Notably, for the OAm-AgTe NFs, we observed a shift of −0.4 eV in the $Ag3d_{5/2}$ and Te3d peaks (see Figure S10).

In exploring other stabilizers to induce fluorescence, our control experiments hint at the critical role that OAm plays in inducing high fluorescence in NFs. For instances, when the nanofibers interacted with hexadecylamine, fluorescence was triggered, which is in marked contrast to the complete absence of fluorescence when treating the nanofibers with 1-decanethiol (Figure S11). It is worth highlighting the residual fluorescence intensity exhibited by hexadecylamine compared to OAm, which seems to manifest an important role of the organic chain in this phenomenon. Furthermore, opting for OAm as a reagent and solvent offers additional advantages. OAm not only ensures effective resuspension of the dried nanofibers, but also promotes a more homogeneous interaction with the entire nanofiber assembly without the need for additional solvent.

The OAm-AgTe NFs demonstrate high stability at room temperature (RT) for extended periods, maintaining their fluorescent emission when stored in OAm. Curiously, when the fluorescent nanofibers are purified in hexane, they also retain their optical response. However, a noticeable tendency for these nanofibers to coalesce into a solid fibrillar structure emerge after a few minutes. Resuspending the nanofibers in other organic solvents allows to maintain colloidal stability without fibrillar coalescence, although this leads to changes in their optical properties, resulting in a reduction or total quenching of their emission (see Figure S12). To enhance colloidal stability and maintain consistent optical properties in solution, the fluorescent nanofibers underwent post-treatment with oleic acid (OA) in hexane, serving as a secondary stabilizing agent [24] (see the experimental section for details). This additional stabilization led to the formation of colloidal-stable nanofibers when dispersed in hexane (see Figure S13).

To complete the study of the photophysical properties of the OA stabilized fluorescent nanofibers (denoted as OA/OAm-AgTe NFs), the UV–vis absorption, emission, and excitation spectra in hexane solution and the emission in the solid state were obtained (Fig. 3). The matching found between the absorption and excitation spectra probes the purity of the samples (Fig. 3A). Moreover, the solution and solid spectra emission are almost coincident, suggesting a similar aggregation effect. The live time excited-state fluorescent spectra were obtained for the OA/OAm-AgTe NFs being a biexponential with two times of 3.23 ns (residual) and a second component with 5.65 ns (Table 1).

Temperature-dependent studies in the solid state were performed following the emission upon exciting at 568 nm, using a fibre optic device connected to the spectrofluorometer to explore the thermostability. Fig. 3B, shows the emission spectra which increase in intensity with the temperature ranging from 25 °C up to 80 °C, and later constantly decreasing from 90 °C to 130 °C. After this temperature ranges, the emission was totally quenched. Figs. 3E-F shows the cooling steep. The fibres were stable enough after cooling (120 °C to 25 °C), recovering *ca.* of 67 % of the initial emission intensity, attributed to probably the rearrangement mode in the solid-state and partial degradation. The temperature-dependent decay analysis shows a notable fitting to minimum square values, suggesting using these nanofibers as a nanothermometer for the ranges of 25–90 °C and 90–120 °C.

In conclusion, this study explores the reactivity of diphenyl ditelluride (DPDT) with $AgNO_3$ in acetonitrile at room temperature under an inert atmosphere. The reaction led to the formation of long nanofibers with a 10–20 nm thickness and intricate nano structure. HR-TEM analysis revealed an alignment of dark areas (Ag and Te) along the nanofibers. Electron diffraction showed a pattern of rings that indicate the formation of small crystalline nanoclusters with an atomic percentage of ca. 53 % of Ag and ca. 47 % of Te. The organometallic nanofibers strongly insulate at room temperature due to an organic insulating shell formed by the phenyl groups. We observed that the organometallic nanofibers acquire a strong fluorescence emission after treatment with oleylamine under an inert atmosphere. These emissive nanofibers can be explored as nano thermometers in the ranges of 25–90 °C and 90–120 °C. Based on our results, it is plausible to propose that oleylamine plays a crucial role in initiating an aggregation process of the nanofibers. This phenomenon is evident in the comparative HR-TEM images at low magnification (Figs. 1A and 2C). Moreover, the interaction with oleylamine induces noteworthy structural alterations within the nanofibers. Notably, the previously internal granular electron-dense nanostructures distinguishable (dark areas related with Ag and Te) shift from a uniform distribution to a more random arrangement. These structural modifications ultimately lead to the development of highly emissive nanofibers. Additional research is warranted to uncover the precise chemical influence that oleylamine exerts on the organometallic

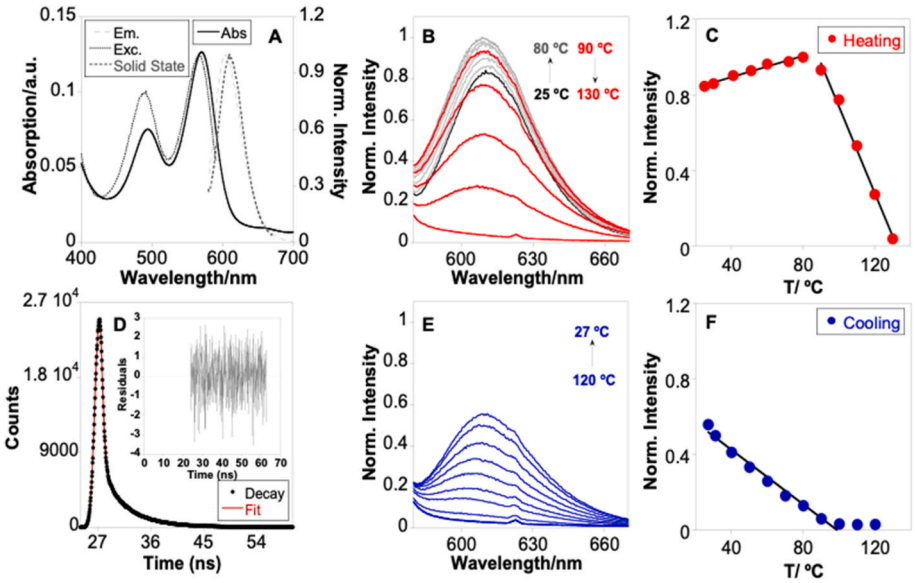

Fig. 3. UV–vis absorption, emission, and excitation spectra in solution as well as the emission spectra in solid state (A). Temperature-dependent emission spectra (B) collected through a warming cycle between 25 °C to 130 °C. $I_{norm.}$ vs. T plot recorded in the emission maximum at 610 nm upon heating [25 to 80 °C (Y = 0.78063 + 0.002818x, yielding R = 0.99067; 90 to 130 °C Y = 3.0273–0.022888x yielding R = 0.99687] (C). Life-time decay and fitting of the OA/OAm-AgTe NFs in hexane, l_{exc} = 568 nm (D). Temperature-dependent emission spectra (E) in a cooling cycle between 120 °C to 27 °C. $I_{norm.}$ vs. T plot recorded in the emission maximum at 610 nm upon cooling [100 to 27 °C (Y = 0.71185–0.0072105x, yielding R = 0.99103)] (F).

Table 1
Absorption in solution (λ_{abs}), emission maximum in solution (λ_{em}), Stokes shift (Dl), emission maximum in the solid state (λ_{em}^{Solid}), and fluorescence lifetime (t) of the purified and oleylamine stabilized fluorescent nanofibers in hexane.

λ_{abs}[nm]	λ_{em}[nm]	Δλ [nm]	λ_{em}^{Solid} [nm]	t[ns]
568	606	285714.29	610	$T_1 = 3.23$ $T_2 = 5.65$

silver-telluride complexes that constitute the nanofibers. An in-depth exploration of the underlying factors that give rise to the remarkably intense fluorescence will permit applied these concepts in designing nanomaterials with enhanced optical responses based on Ag and Te via initial coordination chemistry for various optoelectronic applications.

Author's contributions

J.D., J.F-L, and A.F-L performed the experiments and data analysis of nanofiber synthesis section. B. R. G. perform TEM and HR-TEM analysis. E.B. and S. B. study the nanofibers by HAADF-STEM. F.D and J.F-L performed the experiments related to photophysical studies. H.M.S perform the ESI MS spectrometry studies. A.F. S and L. B. performed the conductivity measurements. J. F. L., C. L., A. d S. conceptualization. J.F-L and C.L. wrote the first manuscript draft. J. F-L, A.F.L, C.L, J.L.C, A.d. S., and H.M.S obtained the funding for the project. All authors contributed to writing and correction of final draft, given approval for the final version of the manuscript.

All authors declare no competing interests.

Declaration of competing interest

The authors declare any conflict of Interest.

Data availability

Data will be made available on request.

Acknowledgements

The authors acknowledge the financial support by the Associate Laboratory Research Unit for Green Chemistry-Clean Processes and Technologies-LAQV which is financed by national funds from FCT/MEC (UID/QUI/50006/2013) and co-financed by the ERDF under the PT2020 Partnership Agreement (POCI-01-0145-FEDER-007265), as well as the PROTEOMASS Scientific Society, General Funds 2022–2023 (Portugal) for funding support.

J.F.-L., A.F.-L.; C.L.; J.D.; and J.L.C.-M. thank the FCT-MEC for the research grant SiSi4Bacter (PTDC/QUI-COL/1517/2020). J. F.-L. thanks FCT-UNL for the research contract through the Program DL 57/2016 Norma Transitória. F.D. thanks to FCT-MEC (Portugal) for his doctoral grant 2021.05161.BD. H.M.S acknowledges the Associate Laboratory for Green Chemistry-LAQV (LA/P/0008/2020) funded by FCT/MCTES for his research contract. A.F.-L. thanks the research contract DL57 associated to the grant SiSi4Bacter (PTDC/QUI-COL/1517/2020).

A. A. Dos Santos thank FAPESP (2014/17310–5, 2016/09579–0 and 2018/24434–3), IQ-USP and CNPq (401797/2013–9) for financial support. L.B. is supported by the US Department of Energy, Basic Energy Sciences program, through award DE-SC0002613. A portion of this work was performed at the National High Magnetic Field Laboratory, which is supported by the National Science Foundation Cooperative Agreement No. DMR-2128556 and the State of Florida. The authors acknowledge financial support from the European Commission under the Horizon 2020 Programme by grant no. 731019 (EUSMI).

Supporting Information

The data that support the findings of this study are available in the SI and from the corresponding author upon reasonable request.

Appendix A. Supplementary data

Supplementary data to this article can be found online at https://doi.org/10.1016/j.dyepig.2023.111754.

References

[1] Brutchey RL. Diorganyl dichalcogenides as useful synthons for colloidal semiconductor nanocrystals. Acc Chem Res 2015;48:2918–26. https://doi.org/10.1021/acs.accounts.5b00362.

[2] Kisker DW, Steigerwald ML, Kometani TY, Jeffers KS. Low-temperature organometallic vapor phase epitaxial growth of CdTe using a new organotellurium source. Appl Phys Lett 1987;50:1681–3. https://doi.org/10.1063/1.97766.

[3] Schlecht S, Budde M, Kienle L. Nanocrystalline tin as a preparative tool: synthesis of unprotected nanoparticles of SnTe and SnSe and a new route to (PhSe) 4 Sn. Inorg Chem 2002;41:6001. https://doi.org/10.1021/ic020272y. 5.

[4] Webber DH, Brutchey RL. Photolytic preparation of tellurium nanorods. Chem Commun 2009;2:5701. https://doi.org/10.1039/b912434a.

[5] Sun F, Hong W, He X, Jian C, Ju Q, Cai Q, et al. Synthesis of ultrathin topological insulator β-Ag_2Te and Ag_2Te/WSe2-based high-performance photodetector. Small 2023;19:1–12. https://doi.org/10.1002/smll.202205353.

[6] Gautam AK, Singh HH, Khare N. Multifunctional flexible Ag_2Te-nylon nanocomposite freestanding film for harvesting thermal and mechanical energy. Nano Energy 2023;107:108125. https://doi.org/10.1016/j.nanoen.2022.108125.

[7] Fernández-Lodeiro J, Rodríguez-González B, Santos HM, Bertolo E, Capelo JL, Dos Santos AA, et al. Unraveling the organotellurium chemistry applied to the synthesis of gold nanomaterials. ACS Omega 2016;1:1314–25. https://doi.org/10.1021/acsomega.6b00309.

[8] Fernández-Lodeiro J, Rodríguez-Gónzalez B, Novio F, Fernández-Lodeiro A, Ruiz-Molina D, Capelo JL, et al. Synthesis and characterization of $PtTe_2$ multi-crystallite nanoparticles using organotellurium nanocomposites. Sci Rep 2017;7:9889. https://doi.org/10.1038/s41598-017-10239-8.

[9] Liaw W-F, Lai C-H, Chiou S-J, Horng Y-C, Chou C-C, Liaw M-C, et al. Synthesis and characterization of polymeric Ag(I)-Telluroether and Cu(I)-Diorganyl ditelluride complexes: crystal structures of $[Ag(MeTe(CH_2)_3TeMe)_2]n[BF_4]_n$, $[(\mu_2\text{-MeTeTeme})Cu(\mu\text{-Cl})]_n$, and $[Ag_2(NCCH_3)_4(\mu2\text{-}(p\text{-}C_6H_4F)TeTe(p\text{-}C_6H_4F))_2][BF_4]_2$. Inorg Chem 1995;34:3755–9. https://doi.org/10.1021/ic00118a024.

[10] Cuerva C, Fernández-Lodeiro J, Cano M, Capelo-Martínez JL, Lodeiro C. Water-soluble hollow nanocrystals from self-assembly of AIEE-active Pt(II) metallomesogens. Nano Res 2021;14:245–54. https://doi.org/10.1007/s12274-020-3078-0.

[11] Chua MH, Chin KLO, Loh XJ, Zhu Q, Xu J. Aggregation-induced emission-active nanostructures: beyond biomedical applications. ACS Nano 2023;17:1845–78. https://doi.org/10.1021/acsnano.2c10826.

[12] Zalmi GA, Jadhav RW, Mirgane HA, Bhosale SV. Recent advances in aggregation-induced emission active materials for sensing of biologically important molecules and drug delivery system. Molecules 2021;27:150. https://doi.org/10.3390/molecules27010150.

[13] Li Y, Xu Z, Zhu X, Chen B, Wang Z, Xiao B, et al. Creation of efficient blue aggregation-induced emission luminogens for high-performance nondoped blue OLEDs and hybrid white OLEDs. ACS Appl Mater Interfaces 2019;11:17592–601. https://doi.org/10.1021/acsami.9b03177.

[14] Liu H, Bai H, Lam JWY, Kwok RTK, Tang BZ. Recent advances in aggregation-induced emission materials for enhancing solar energy utilization. Nanoscale Horizons 2023;8:453–9. https://doi.org/10.1039/D2NH00506A.

[15] dos Santos SS, Cabral BN, Abram U, Lang ES. Bis(4-pyridyl)ditelluride as starting material for the synthesis of zwitterionic compounds and metal complexes. J Organomet Chem 2013;723:115–21. https://doi.org/10.1016/j.jorganchem.2012.09.007.

[16] Lodeiro C, Bastida R, de Blas A, Fenton DE, Macías A, Rodríguez A, et al. Complexes of lead(II) and lanthanide(III) ions with two novel 26-membered-imine and -amine macrocycles derived from 2,6-bis(2-formylphenoxymethyl)pyridine. Inorg Chim Acta 1998;267:55–62. https://doi.org/10.1016/S0020-1693(97)05552-7.

[17] Carrera EI, Seferos DS. Semiconducting polymers containing tellurium: perspectives toward obtaining high-performance materials. Macromolecules 2015;48:297–308. https://doi.org/10.1021/ma502307b.

[18] Mathur PC, Dawar AL, Taneja OP. Electrical transport properties of copper-doped tellurium films. Thin Solid Films 1980;66:281–5. https://doi.org/10.1016/0040-6090(80)90382-X.

[19] Yang M, Su T, Li S, Li S, Hu M, Liu X. Facile synthesis and high thermoelectric performance of tellurium with antimony doping. J Alloys Compd 2021;887:161342. https://doi.org/10.1016/j.jallcom.2021.161342.

[20] Fan F, Wang L, Li F, Fu Y, Xu H. Stimuli-responsive layer-by-layer tellurium-containing polymer films for the combination of chemotherapy and photodynamic therapy. ACS Appl Mater Interfaces 2016;8:17004–10. https://doi.org/10.1021/acsami.6b04998.

[21] Stinespring CD, Freedman A. Thermal and photolytic decomposition of adsorbed cadmium and tellurium alkyls. MRS Proc 1988;129:57. https://doi.org/10.1557/PROC-129-57.

[22] Hadiyawarman Eguchi M, Tanaka H. Control of the neuromorphic learning behavior based on the aggregation of thiol-protected Ag-Ag2S core-shell nanoparticles. Jpn J Appl Phys 2020;59. https://doi.org/10.7567/1347-4065/ab5c77.

[23] Barkoula NM, Alcock B, Cabrera NO, Peijs T. Flame-retardancy properties of intumescent ammonium poly(phosphate) and mineral filler magnesium hydroxide in combination with graphene. Polym Polym Compos 2008;16:101–13. https://doi.org/10.1002/pc.

[24] Mourdikoudis S, Menelaou M, Fiuza-Maneiro N, Zheng G, Wei S, Pérez-Juste J, et al. Oleic acid/oleylamine ligand pair: a versatile combination in the synthesis of colloidal nanoparticles. Nanoscale Horizons 2022;7:941–1015. https://doi.org/10.1039/D2NH00111J.